HHS Public Access

Author manuscript

J Am Chem Soc. Author manuscript; available in PMC 2019 March 14.

Published in final edited form as:

J Am Chem Soc. 2018 March 14; 140(10): 3505–3509. doi:10.1021/jacs.7b13307.

Active Probes for Imaging Membrane Dynamics of Live Cells with High Spatial and Temporal Resolution over Extended Timescales and Areas

Huaimin Wang[†], **Zhaoqianqi Feng**[†], **Steven J. Del Signore**[≠], **Avital A. Rodal**[≠], and **Bing Xu**[†,*]

[†]Department of Chemistry, Brandeis University, 415 South Street, Waltham, MA 02453, USA

[≠]Department of Biology, Brandeis University, Waltham MA 02454, USA

Abstract

Despite the advancement of molecular imaging techniques, there is an unmet need of probes for directly imaging membrane dynamics of live cells. Here we report a novel type of active (or enzyme responsive) probes to directly image membrane dynamics of live cells with high spatial and temporal resolution over extended timescales and areas. Because lipid rafts enrich cholesterols and GPI-anchored enzymes (e.g., ectophosphatases), we design probes that consist of an enzymatic trigger, a fluorophore, and a cholesterol that are affinitive to cell membrane. Being water soluble and as the substrate of ectophosphatase, these cell compatible probes preferentially and rapidly assemble in plasma membrane, exhibit strong fluorescence, work at micromolar concentrations, and easily achieve high resolution monitoring of nanoscale heterogeneity in membranes of live cells, the release of exosomes, and the membrane dynamics of live cells. This work provides a facile means to link membrane dynamics and heterogeneity to cellular processes for understanding the interactions between membranes and proteins.

TOC image

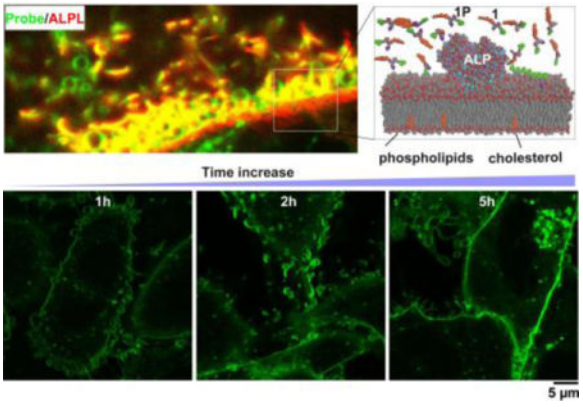

*Corresponding Author: bxu@brandeis.edu.

Supporting Information

The details of the synthesis, methods, original cell toxicity results, antibody stating and other figures. This material is available free of charge via the Internet at http://pubs.acs.org

Although gaining increasing support by recent studies, the membrane raft ("lipid rafts") hypothesis[1] remains controversial due to the lack of suitable imaging probes.[2] Considerable efforts have focused on proving the existence of lipid rafts or studying membrane dynamics with a variety of techniques, including photoactivated localization microscopy (PALM), stimulated emission depletion (STED), and interferometric scattering microscopy (ISCAT).[3] Recently, Nile Red was used as a probe for super-resolution membrane imaging based on stochastic optical reconstruction microscopy (STORM) to reveal the heterogeneity of membrane,[4] but it still has low temporal resolution (minute). In fact, none of these approaches matches well to the dynamic nature of membranes in live cells.[5] Fluorescent probes that specifically label rafts or non-raft domains have been used to probe nanoscale heterogeneity in live-cell membranes and to distinguish different membrane compartments.[6] Genetic methods that rely on red fluorescent protein (RFP)/green fluorescent protein (GFP) fusion are widely used for exploring the dynamics of live cell membrane.[7] While these methods have provided many valuable insights into how cellular membranes are heterogeneous and form distinct and highly ordered domains along with less organized and more fluid regions, each of them still poorly matches with the dynamic nature of lipid rafts or membranes. Particularly, there is still an unmet need of probes for directly imaging membrane dynamics of live cells with high spatial and temporal resolution over extended timescales and large areas.[2]

To address the aforementioned need, we choose to develop active (or enzyme responsive) probes using the emerging approach of integrating enzymatic reaction and molecular assembly that has found applications in many areas,[8] including molecular imaging.[9] Because lipid rafts enrich cholesterols[10] and GPI-anchored enzymes (e.g., ectophosphatases[11]), we design these novel active and raft-affinitive probes consisting of an enzymatic trigger, a fluorophore, and a cholesterol. Being water soluble and as the substrate of ectophosphatase, the probes preferably and rapidly assemble in the membrane to exhibit strong fluorescence. Such cell compatible, active probes work at micromolar concentrations, require short incubation period, and easily achieve high resolution monitoring of nanoscale heterogeneity in live-cell membranes. Using the probes, we observe heterogeneity of one cell membrane, dynamic movement of lipid rafts on different cells, release of exosomes, membrane dynamic during cell death, and membranes in 3D cell spheroids. Moreover, immunofluorescence staining indicates the co-localization of this probe with nanoclusters of GPI anchored proteins. Our results confirmed the nanoscale heterogeneity of membrane and the existence of interconnectivity at the nanoscale between live cells. The active probes, being suitable for live cell imaging by conventional fluorescent microscope, yield reproducible results, match well with the dynamic nature of cell membrane, and provide a facile means to link membrane heterogeneity to a diverse range of cellular processes.

Figure 1 shows the molecular design of the representative active probe (**1P**), which consists of three parts: i) cholesterol, a basic component of the cell membrane that not only maintains cell homeostasis and constructs lipid rafts, but also plays crucial roles in cell functions;[12] ii) phosphotyrosine, a substrate of an ectoenzyme (i.e., ubiquitous alkaline phosphatase (ALPL) believed to co-localize with lipid rafts[13]) that enables an enzymatic reaction on cell surface; iii) 4-nitro-2,1,3-benzoxadiazole (NBD), an environment-sensitive fluorophore that reports

molecular self-assembly since this fluorophore exhibits bright fluorescence in hydrophobic environment.[14] Upon the treatment of phosphatase, **1P** turns into **1**, which forms fluorescent supramolecular assemblies. At lower concentration that below CMC, most of converted **1** could be quickly uptake by cells or diffuse away, which exhibit very weak fluorescence. At the concentration above CMC, **1P** likely interacts with cell membrane as a continuum,[15] which is as monomers, dimers, or multimers. Such a continuum further self-assembles through enzyme induced transformation of **1P** to **1**. In this process, the activity of GPI anchored ALPL plays crucial role for maintain the assemblies that likely consist of **1P** and **1**.

The CMC of **1P** is 3.3 μM (Figure S1), which suggest **1P** also has good self-assembly ability. As revealed by the dephosphorylation experiment (Figure S2), **1P** undergoes ALP catalyzed dephosphorylation, which exhibited two stages. At first 4h, **1P** undergoes fast dephosphorylation after the treatment of ALP. With the increment of time, the percentage of conversion changes little, suggesting that the nanostructures formed mainly by **1** likely incorporate the precursors (**1P**) to hinder the complete dephosphorylation. After demonstrated enzyme induced self-assembly of **1P** in vitro (Figure. S3A to C) by TEM, we incubate **1P** with Saos-2 cells and observe distinctive domains (i.e., raft-like structures[5]) of different sizes on the cell membrane. The fluorescence of active probe mainly localizes on the cell membrane with different intensities on single cell or many cells (i.e., a large area[2]), less on cell organelles with increased incubation time (Figure 2A, movie S1). Without the enzymatic trigger (i.e., the phosphate on tyrosine), **1** shows little fluorescence (Figure 2B). However, after being generated from **1P** in-situ in lipid rafts, the assemblies of **1**, as the probes, exhibit bright fluorescence and achieve excellent resolution to reveal the heterogeneity of the membrane (Figures 2C, S5 and S6), and permit observing the size distribution of the domains on the membrane (Figure 2D). Contrary to the imaging result, **1P** exhibits higher intensity in fluorescent spectra (Figure S3D to F) than 1P plus ALP does. This observation agrees with that **1P** is more soluble than **1**, which results in less fluorescent quenching, as previously explained.[14] These results confirm the unique advantage of the active probes. Live cell imaging shows lateral mobility of membrane domains and dynamics within 100 seconds (Figure 2E, movie S2), which indicate membrane domains fluctuating during lateral movement. Membrane domains in different regions (arrows in Figure 2E) show distinctive fluctuation, reflecting heterogeneity and dynamic of membrane domains. Saos-2 cells treated by **1P** with exogenous ALPs or two well-known uncompetitive inhibitors of ALPL (i.e., levamisole[16] or DQB[17]) show weaker fluorescence than the control cells (Figure S7). These results, indeed, confirm that the EISA, as an in situ process, is critical for membrane imaging. Detailed cellular distribution experiments indicate that **1P** localizes with some organelles with membrane structures (lysosome and Golgi, Figures S8 to S11) only after long time incubation. Moreover, the active probe can also be metabolized during the passage of the cells (Figure S12), which further demonstrate the biocompatibility of the probe.

The antibody to GPI-anchored ALPL mainly co-localized with assemblies of active probe (Figure 3A). Matrix vesicles (i.e., exosomes[18]) extruded from plasma membrane are clearly observable, and immunofluorescence also reveals that the vesicles encapsulate ALPL

(Figure 3B), agreeing with previous findings that Saos-2 cells secret matrix vesicles containing ALPL.[19] We also perform immunofluorescent staining without adding mild detergent to permeabilize the cell membrane. The results (Figure S13) suggested that the assemblies of the probe co-localized with ALPL on the extracellular side of plasma membrane. These results together indicate the assemblies of the probe likely distribute in the cell membrane. Since a key feature of lipid rafts is dynamic clustering of cholesterol molecules, the formation of **1** near ALPL in lipid rafts, which generates the dynamic continuum consisting of **1** and **1P**, likely would augment lipid rafts. Using L-amino acid to replace the D-amino acid generates L-**1P**, which shows similar phenomenon (Figure 3C&D) as that of **1P**. In contrast, commercial cholesterol-containing probes, such as 3-hexanoyl-NBD cholesterol[20] (Figure 3E) and NBD-cholesterol[20] (Figure 3F), though used for investigating lipid transport processes as well as lipid-protein interactions, are unable to reveal the dynamics of cell membrane: the former hardly shows fluorescence at same condition as that of using **1P**; the latter largely distributes in cytoplasm. Replacing phosphorylated tyrosine with phosphorylated serine generates **2P** (Scheme S1), which exhibits fluorescent puncta in entire Saos-2 cells (Figure S14), further demonstrating the designed active probe is an enzyme specific probe. Moreover, **1P** diffuses into 3D cell spheroids and reveals cell-cell junctions in the 3D cell spheroid (Figure 3G, movie S3), confirming the active probes are applicable for observing membrane dynamics over not only a large area, but also a large volume.

We also apply **1P** on eight other human cell lines including six cancer cell lines and two normal cell lines (Figures 4A and S15 to S17). The results indicate that the active probe is a robust imaging probe for studying the heterogeneity and dynamics of membrane over large area and extended time for various cells. Moreover, live cell imaging (movie S4) reveals membrane dynamics of cancer cells (Saos-2) in responding to an anticancer drug candidate, [8f] which disrupts the cytoskeleton and changes the morphology of cell membrane (Figure 4B and Scheme S2), suggesting this active probe reflects membrane dynamics and the heterogeneity in a highly complex condition (e.g., cells under insult).

In conclusion, our results confirm the nanoscale heterogeneity of membranes and the existence of membrane interconnectivity at the nanoscale between live cells. Because the active probes are suitable for conventional fluorescent microscope, yield reproducible results, match well with the dynamics of cell membrane over extended timescales and large areas, we anticipate that they will provide a facile means to link membrane dynamics and heterogeneity to cellular processes for understanding the interactions between membranes and proteins.[21] For example, it may act as a tool for understanding the role of lipid rafts in endocytosis[22] or exocytosis[23] in real time. Moreover, the principle of active probes may be useful for developing imaging probes for super-resolution microscopy or for understanding dynamic self-assembling processes.[24]

Supplementary Material

Refer to Web version on PubMed Central for supplementary material.

Acknowledgments

This work was partially supported by NIH (CA142746), NSF (DMR-1420382) and W. M. Keck Foundation. ZF thanks the Dean's fellowship.

References

1. Simons K, Ikonen E. Nature. 1997; 387:569. [PubMed: 9177342]
2. Sezgin E, Levental I, Mayor S, Eggeling C. Nat Rev Mol Cell Biol. 2017; 18:361. [PubMed: 28356571]
3. a) Sengupta P, Jovanovic-Talisman T, Skoko D, Renz M, Veatch SL, Lippincott-Schwartz J. Nat Methods. 2011; 8:969. [PubMed: 21926998] b) de Wit G, Danial JS, Kukura P, Wallace MI. Proc Natl Acad Sci. 2015; 112:12299. [PubMed: 26401022] c) Saka SK, Honigmann A, Eggeling C, Hell SW, Lang T, Rizzoli SO. Nat Commun. 2014; 5d) Eggeling C, Ringemann C, Medda R, Schwarzmann G, Sandhoff K, Polyakova S, Belov VN, Hein B, von Middendorff C, Schönle A. Nature. 2009; 457:1159. [PubMed: 19098897]
4. Moon S, Yan R, Kenny SJ, Shyu Y, Xiang L, Li W, Xu K. J Am Chem Soc. 2017; 139:10944. [PubMed: 28774176]
5. Komura N, Suzuki KG, Ando H, Konishi M, Koikeda M, Imamura A, Chadda R, Fujiwara TK, Tsuboi H, Sheng R. Nat Chem Biol. 2016; 12:402. [PubMed: 27043189]
6. Baumgart T, Hunt G, Farkas ER, Webb WW, Feigenson GW. BBA BIOMEMB. 2007; 1768:2182.
7. Snapp E. Curr Protoc Cell Biol. 2005; 21(4):1.
8. a) Du X, Zhou J, Shi J, Xu B. Chem Rev. 2015; 115:13165. [PubMed: 26646318] b) Pires RA, Abul-Haija YM, Costa DS, Novoa-Carballal R, Reis RL, Ulijn RV, Pashkuleva I. J Am Chem Soc. 2015; 137:576. [PubMed: 25539667] c) Takaoka Y, Sakamoto T, Tsukiji S, Narazaki M, Matsuda T, Tochio H, Shirakawa M, Hamachi I. Nat Chem. 2009; 1:557. [PubMed: 21378937] d) Tanaka A, Fukuoka Y, Morimoto Y, Honjo T, Koda D, Goto M, Maruyama T. J Am Chem Soc. 2015; 137:770. [PubMed: 25521540] e) Feng Z, Wang H, Zhou R, Li J, Xu B. J Am Chem Soc. 2017; 139:3950. [PubMed: 28257192] f) Feng Z, Wang H, Chen X, Xu B. J Am Chem Soc. 2017; 139:15377. [PubMed: 28990765]
9. a) Razgulin A, Ma N, Rao J. Chem Soc Rev. 2011; 40:4186. [PubMed: 21552609] b) Gao W, Xing B, Tsien RY, Rao J. J Am Chem Soc. 2003; 125:11146. [PubMed: 16220906] c) Xing B, Khanamiryan A, Rao J. J Am Chem Soc. 2005; 127:4158. [PubMed: 15783183] d) Liang G, Ren H, Rao J. Nat Chem. 2010; 2:54. [PubMed: 21124381]
10. Rajendran L, Simons K. J Cell Sci. 2005; 118:1099. [PubMed: 15764592]
11. a) Parton RG, Joggerst B, Simons K. J Cell Biol. 1994; 127:1199. [PubMed: 7962085] b) Fonta C. Chem. 2016; 1:184.
12. Simons K, Ikonen E. Science. 2000; 290:1721. [PubMed: 11099405]
13. Ermonval, M., Baychelier, F., Fonta, C. Neuronal Tissue-Nonspecific Alkaline Phosphatase (TNAP). Springer; 2015. p. 167
14. Gao Y, Shi J, Yuan D, Xu B. Nat Commun. 2012; 3:1033. [PubMed: 22929790]
15. a) Feng Z, Zhang T, Wang H, Xu B. Chem Soc Rev. 2017; 46:6470. [PubMed: 28849819] b) Wang H, Shi J, Feng Z, Zhou R, Wang S, Rodal AA, Xu B. Angew Chem, Int Ed. 2017; 56:16297.
16. Borgers M. J Histochem Cytochem. 1973; 21:812. [PubMed: 4741290]
17. Dahl R, Sergienko EA, Su Y, Mostofi YS, Yang L, Simao AM, Narisawa S, Brown B, Mangravita-Novo A, Vicchiarelli M. J Med Chem. 2009; 52:6919. [PubMed: 19821572]
18. a) György B, Szabó TG, Pásztói M, Pál Z, Misják P, Aradi B, László V, Pállinger É, Pap E, Kittel Á. Cell Mol Life Sci. 2011; 68:2667. [PubMed: 21560073] b) Valadi H, Ekström K, Bossios A, Sjöstrand M, Lee JJ, Lötvall JO. Nat Cell Biol. 2007; 9:654. [PubMed: 17486113] c) Wan S, Zhang L, Wang S, Liu Y, Wu C, Cui C, Sun H, Shi M, Jiang Y, Li L. J Am Chem Soc. 2017; 139:5289. [PubMed: 28332837]
19. Morris DC, Masuhara K, Takaoka K, Ono K, Anderson HC. Bone Miner. 1992; 19:287. [PubMed: 1472898]

20. Haldar, S., Chattopadhyay, A. Fluorescent Methods to Study Biological Membranes. Springer; 2012. p. 37

21. van den Bogaart G, Meyenberg K, Risselada HJ, Amin H, Willig KI, Hubrich BE, Dier M, Hell SW, Grubmüller H, Diederichsen U. Nature. 2011; 479:552. [PubMed: 22020284]

22. a) Schöneberg J, Lehmann M, Ullrich A, Posor Y, Lo WT, Lichtner G, Schmoranzer J, Haucke V, Noé F. Nat Commun. 2017; 8b) Scita G, Di Fiore PP. Nature. 2010; 463:464. [PubMed: 20110990]

23. a) Cary LA, Cooper JA. Nature. 2000; 404:945. [PubMed: 10801110] b) Di Paolo G, De Camilli P. Nature. 2006; 443:651. [PubMed: 17035995]

24. a) Liang Y, Lynn DG, Berland KM. J Am Chem Soc. 2010; 132:6306. [PubMed: 20397724] b) Liang C, Ni R, Smith JE, Childers WS, Mehta AK, Lynn DG. J Am Chem Soc. 2014; 136:15146. [PubMed: 25313920] c) Debnath S, Roy S, Ulijn RV. J Am Chem Soc. 2013; 135:16789. [PubMed: 24147566] d) Li J, Nowak P, Otto S. J Am Chem Soc. 2013; 135:9222. [PubMed: 23731408] e) Ashkenasy G, Hermans TM, Otto S, Taylor AF. Chem Soc Rev. 2017; 46:2543. [PubMed: 28418049]

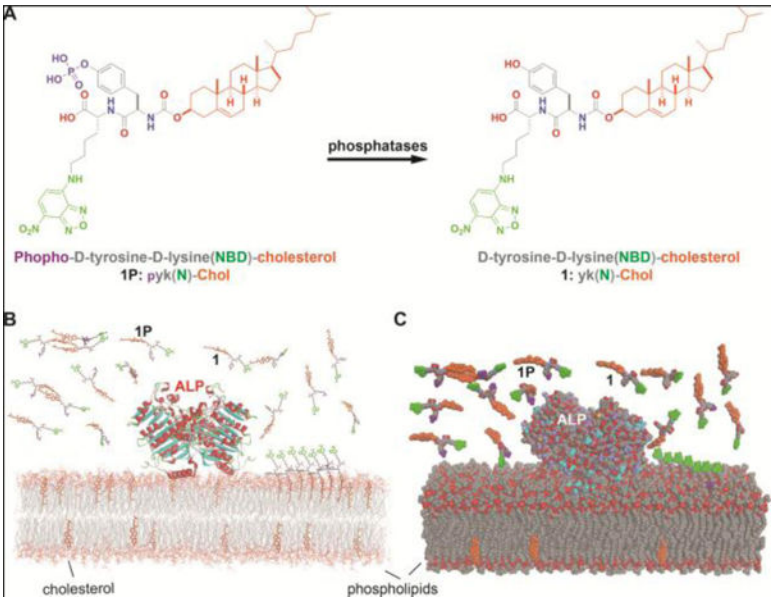

Figure 1.

(A) Molecular structure of a representative active probe, **1P**, which contains cholesterol (orange), fluorophore of NBD (green), and phospho-D-tyrosine. Illustrations of enzymatic instructed self-assembly of **1P** to form assemblies of **1** that anchor in cell membranes in (B) stick and (C) CPK models.

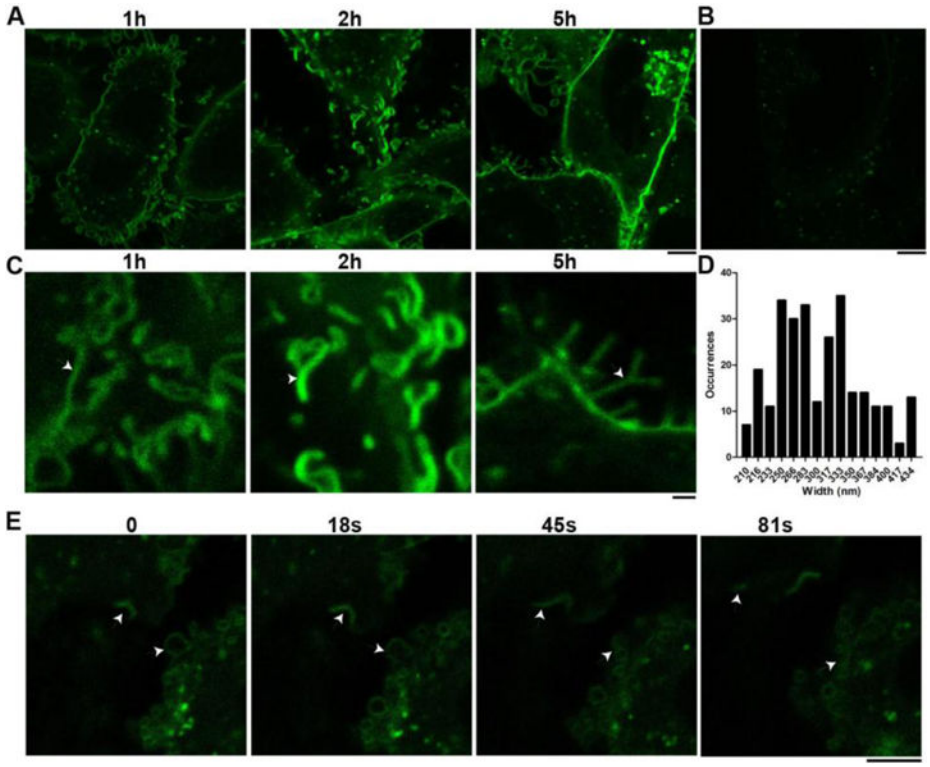

Figure 2.

CLSM (ZEISS LSM 880) images of Saos-2 cells treated with (A) **1P** at the concentration of 25 μM for 1, 2 and 5 h and (B) **1** (25 μM) for 5 h. Scale bar is 5 μm. (C) Magnification of CLSM images in (A), scale bar is 1 μm. (D) Size distribution of individual membrane domain structures as indicated by arrow in (C). (E) Spatiotemporal dependent changes of membrane domains within 90s. After treating Saos-2 cells with **1P** (10 μM) for 1 h, we changed the medium with fresh culture medium and then observed the cells by CLSM. Scale bar is 5 μm. Arrow in (C) and (E) indicates the membrane domains of Saos-2 cells.

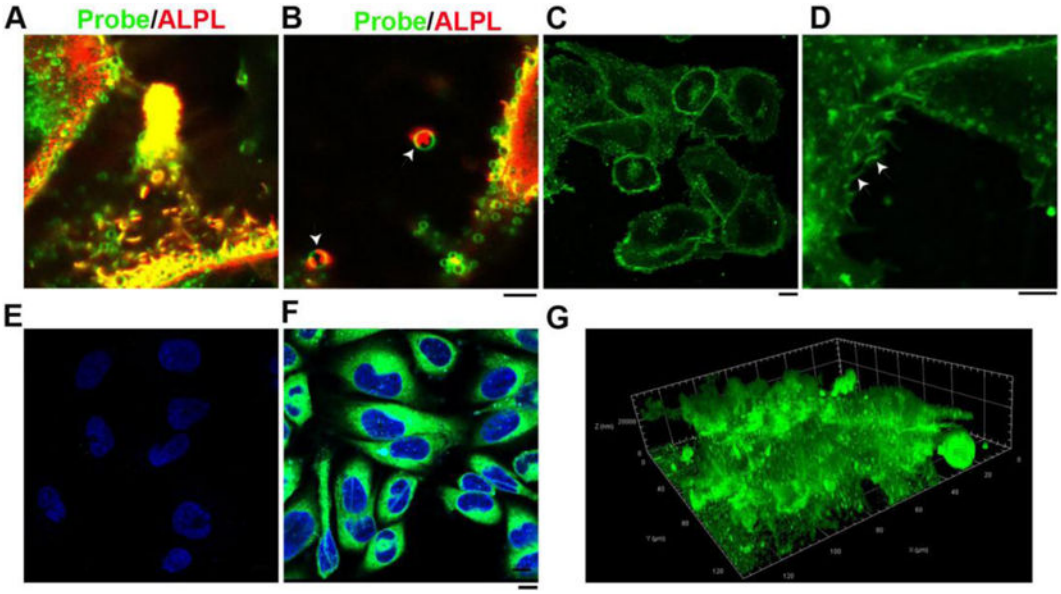

Figure 3.

(A) Saos-2 cells treated with **1P** (25 μM, 2 h) and then analyzed by immunofluorescence for ALPL (red represents antibodies). Pearson's R value is 0.65 from 20 cells. (B) Matrix vesicles secreted by Saos-2 cells containing ALPL; scale bar is 5 μm. (C) and (D) CLSM images of Saos-2 cells treated with L-**1P** at the concentration of 25 μM for 2 h; scale bar in (C) is 10 μm and (D) is 5 μm. CLSM images of Saos-2 cells treated with (E) 3-hexanoyl-NBD cholesterol (25 μM, 2 h) and (F) NBD cholesterol (25 μM, 2h); scale bar is 10 μm. (G) 3D reconstruction of HS-5 cell spheroids treated with **1P** (10 μM) for 1 h.

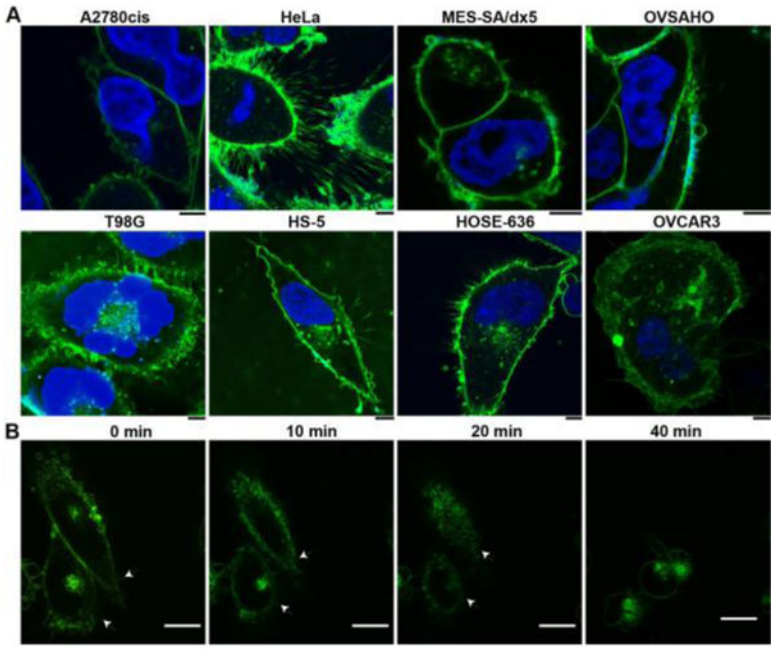

Figure 4.

(A) CLSM images of **1P** (25 μM) treated with other human cell lines for 1 h; scale bar is 5 μm. (B) Time course of CLSM images of Saos-2 cells incubated with **1P** (10 μM) for 1 h and then treated with an anti-cancer drug candidate (50 μM) for 40 minutes. Arrows indicate the changes of membrane rafts. Scale bar is 15 μm.